



*Citation for published version:*

Cetiner, I & Shea, AD 2018, 'Wood waste as an alternative thermal insulation for buildings', *Energy and Buildings*, vol. 168, pp. 374-384. <https://doi.org/10.1016/j.enbuild.2018.03.019>

*DOI:*

[10.1016/j.enbuild.2018.03.019](https://doi.org/10.1016/j.enbuild.2018.03.019)

*Publication date:*

2018

*Document Version*

Peer reviewed version

[Link to publication](#)

*Publisher Rights*

CC BY-NC-ND

## University of Bath

### General rights

Copyright and moral rights for the publications made accessible in the public portal are retained by the authors and/or other copyright owners and it is a condition of accessing publications that users recognise and abide by the legal requirements associated with these rights.

### Take down policy

If you believe that this document breaches copyright please contact us providing details, and we will remove access to the work immediately and investigate your claim.

1 **Wood waste as an alternative thermal insulation building material solution**

2

3 Ikbal Cetiner<sup>a\*</sup>

4 Andrew D. Shea<sup>b</sup>

5

6 <sup>a\*</sup> Istanbul Technical University, Faculty of Architecture, Department of Architecture

7 Postal address: Istanbul Technical University, Faculty of Architecture, Taskisla, Taksim, 34437 Istanbul, Turkey.

8 Telephone number: +90 212 293 1300

9 E-mail address: ikbalcetiner@yahoo.com, cetinerikb@itu.edu.tr

10

11 <sup>b</sup> University of Bath, Department of Architecture and Civil Engineering

12 Postal address: University of Bath, Department of Architecture and Civil Engineering, Bath, BA2 7AY, UK.

13 Telephone number: +44 (0) 1225 386158

14 E-mail address: a.shea@bath.ac.uk

15

16 \*Corresponding author

17

18

19

20

21

22

23

24

25

26

27

28

29

30

31

32

33

## 34 **Wood waste as an alternative thermal insulation building material solution**

35

### 36 **Abstract**

37 Current insulation materials in the construction market, which are predominantly inorganic materials, have a high  
38 performance in relation to heat transfer, i.e. high R-values, but the environmental impacts in their production  
39 processes are significant. The use of bio-based natural fibre materials such as cork, cotton, wood fibre, hemp, etc.  
40 with their lower embodied energy, moisture buffering capacity and, consequently, improved Indoor Environmental  
41 Quality have received increasing focus in both research and application, particularly amongst environmentally-  
42 conscious clients and designers.

43 In this study a natural fibre material in the form of wood waste is examined experimentally to assess its suitability for  
44 use as a thermal insulation material, without the addition of any binder, within a timber frame wall construction. The  
45 wood waste is from primary production sources using untreated material. According to our experimental results, the  
46 thermal conductivity values of wood waste with different densities, ranged from 0.048 to 0.055 W/mK. These values  
47 are slightly higher than commonly used inorganic based insulation materials, although comparable to other natural  
48 insulation materials in the market, but have the economic advantage of being a low-cost by-product. The values  
49 relating to the material hygric performance including the water vapour diffusion resistance factor, water vapour  
50 permeability, and water absorption coefficient were also determined and presented, which will help facilitate future  
51 hygrothermal modelling.

### 52 **Keywords**

53 Wood waste, Thermal Insulation, Natural Building Materials, Hygrothermal.

54

### 55 **1. Introduction**

56 Buildings and the construction industry are major contributors to global CO<sub>2</sub> emissions through embodied and  
57 operational energy use. The industry is a major consumer of natural resources and many products contain materials  
58 that are detrimental to the indoor environment and human health (Pacheco-Torgal *et al.*, 2012). One of the most  
59 effective measures to reduce operational energy use is to insulate the building envelope, which confers benefits in  
60 both heating and cooling energy use. Current thermal insulation materials in the construction market are generally  
61 inorganic materials e.g. extruded polystyrene (XPS), expanded polystyrene (EPS), polyisocyanurate and  
62 polyurethane foam. These materials have a high performance in resisting heat transfer but the environmental impact  
63 of their production processes is high. Accordingly, the use of natural materials, which undergo minimal production  
64 processing, for application as building insulation is an important aspect in the creation of a healthy and sustainable  
65 environment.

66 Recently, many studies have been conducted into the use of bio-based/natural fibre insulation materials as a  
67 replacement for inorganic materials. Bio-based, i.e. plant- or animal-based, insulation materials are a novel class of  
68 insulation materials which include products such as cork, cotton, wood fibre, flax, hemp, coconut, cellulose, rice,  
69 sheep's wool and others. The plant-based materials sequester atmospheric carbon dioxide through photosynthesis  
70 and consequently their use in construction can reduce the net embodied carbon dioxide of a building (Lawrence *et*  
71 *al.*, 2013). When used appropriately, these materials can deliver thermal and acoustic insulation performance  
72 comparable to other insulation materials, but with a lower, or potentially negative, carbon footprint and fewer health  
73 issues during installation (Sutton *et al.*, 2011). Moreover, they have hygroscopic properties, which have positive  
74 effects on building energy consumption (Osanyintola and Simonson, 2006), HVAC system energy consumption in  
75 dwellings (Steeman *et al.*, 2009; Woloszyn *et al.*, 2009) and indoor air quality in buildings (Simonson *et al.*, 2002).  
76 Hygroscopic materials exposed to room air equilibrate indoor humidity through their ability to absorb, store, and  
77 release water vapour from the air (Korjenic *et al.*, 2010; Simonson *et al.*, 2004; Shea *et al.*, 2012). This property  
78 favourably influences the indoor air humidity, primarily in winter when prolonged periods of low indoor air humidity  
79 may be experienced (Korjenic *et al.*, 2011), and reduces the potential for mould growth (Hall, 2010).

80 In the following studies, the use of natural fibre insulation materials without the addition of any binder is discussed  
81 and their mechanical, thermal or hygrothermal characteristics are presented. Zhou *et al.* (2010) developed a  
82 binderless cotton stalk fibreboard (BCSF) from cotton stalk fibres without resins and other chemical additives by hot-  
83 pressing. The boards were produced at densities of 150–450 kg/m<sup>3</sup> and achieved thermal conductivity values ranging  
84 from 0.0585 to 0.0815 W/mK, which are close to those of expanded perlite and vermiculite within the same density  
85 range. Korjenic *et al.* (2011) investigated the use of jute, flax, and hemp for use in the development of novel insulating  
86 materials made from renewable resources and reported comparable thermal and mechanical properties to those of  
87 established conventional insulation materials such as mineral wool, polystyrene and polyurethane. Panyakaew and  
88 Fotios (2011) developed two low density thermal insulation boards, one made from coconut husk and another from  
89 bagasse, both formed without the use of chemical binding additives. The results of their experimental study indicated  
90 that both insulation boards had thermal conductivity values ranging from 0.046 to 0.068 W/Mk which, at the lower  
91 end, were close to those of conventional insulation materials such as mineral wool. Zach *et al.* (2012) conducted a  
92 series of measurements to evaluate the thermal performance and application of sheep's wool insulation. Results  
93 indicated that the sheep's wool had comparable thermal performance to mineral/rock wool. Furthermore, the ability  
94 of sheep's wool to absorb moisture helped to prevent condensation, regulate humidity, and created a pleasant indoor  
95 atmosphere. Briga-Sá *et al.* (2013) experimentally studied the potential applicability of woven fabric waste (WFW)  
96 and a waste of this residue, named woven fabric sub-waste (WFS), as thermal insulation for use in construction. The  
97 results showed that the WFW had better insulation characteristics than the WFS, and the thermal conductivity value  
98 of WFW was similar to the conventional thermal insulation materials, such as expanded polystyrene, extruded

99 polystyrene and mineral wool. Charca *et al.* (2015) studied the thermal properties of Ichu, which is an Andean feather  
100 grass, as a local and cheap natural insulation material for rural dwellings. The results revealed that the thermal  
101 conductivity varied from 0.047 to 0.113 W/mK for mats with unidirectional oriented fibres. Wei *et al.* (2015)  
102 investigated the effect of high frequency heating, board density, particle size and ambient temperature on the  
103 properties of a new thermal insulation material made from rice straw. The results indicated that the optimum physical  
104 and mechanical properties of the boards were obtained with a moisture content of 14% and board density of 250  
105 kg/m<sup>3</sup>. Additionally, the thermal insulation boards had good thermal performance, recording a thermal conductivity in  
106 the range of 0.051 to 0.053 W/mK.

107 These studies highlight that natural building materials are increasingly being investigated as viable thermal insulation  
108 materials for the external envelope of new and existing buildings. The highlighted studies focused primarily on thermal  
109 and mechanical properties of these materials; few of them considered their hygric behaviour.

110 In this paper, the use of Wood Waste (WW) as an insulation material for building envelopes is investigated and  
111 characterisation of its thermal and hygric performance is reported. WW is a common by-product of construction and  
112 demolition, packaging, municipal activities, joinery and furniture manufacture (DEFRA, 2013). The use of this material  
113 within timber frame wall construction, without the addition of binder, facilitates improved management of wood waste,  
114 ease of recycling, and potentially healthier indoor environments. At the present time, wood fibers are used in the  
115 production of wood fibre insulation boards by adding low quantities of PUR resin in a dry process. In this case, the  
116 thermal conductivity values of the boards range between 0.037-0.05 W/mK (GUTEX,2015); however, this production  
117 process also requires a large amount of energy (HPBP, 2017). The use of wood waste received from local sawmills  
118 without treating will reduce energy use and relatedly carbon dioxide release.

119 Wood waste can be defined as a material that has been used for some time and then disposed by the users as well  
120 as the residues from primary wood processing such as sawdust (Alf-Cemind, 2017). In this study, the properties of  
121 the wood waste from primary production sources using untreated material are examined. These residues are  
122 industrial wastes generated by either sawmills and other millwork companies, which are primary wood product  
123 manufacturers, or companies that use products from wood materials milled by primary wood, which are secondary  
124 wood product manufacturers. The primary wood manufacturers produce a variety of WW including bark, chips,  
125 edgings, sawdust, and slabs. These residues typically have a moisture content of 40 to 50 percent. The secondary  
126 wood product industries produce a variety of WW including chips, ends, and sawdust. The moisture content of these  
127 wastes varies considerably because both green, harvested wood and kiln-dried wood are used in secondary  
128 manufacturing. An average moisture content of 45 percent is commonly used in the wood energy industry (EPA,  
129 1996).

130 Our paper reports the characterisation of the aforementioned WW from experimental testing of samples under a  
131 range of environmental conditions as this is necessary to assess the performance of a thermal insulation material  
132 used in the building envelope.

## 133 **2. Hygrothermal Behaviour**

134 The assessment of building envelopes subject to temperature and moisture gradients is a prerequisite in the  
135 investigation of building energy efficiency and the evaluation and creation of a comfortable indoor environment (Moon  
136 *et al.*, 2014). If such environmental conditions are not assessed with a holistic approach and appropriate solutions  
137 integrated into the building design, the resulting building may suffer from excess energy use through increased heat  
138 transmission coefficients of the building envelope elements. The building may also experience structural damage  
139 from interstitial condensation and elevated moisture content, e.g. leading to timber decay, or surface condensation  
140 damage in the form of mould which will lead to poor indoor air quality and an unhealthy environment. The building  
141 element or zone response to temperature and moisture gradients is generally referred to as 'Hygrothermal behaviour'.  
142 This behaviour considers the simultaneous and inter-dependent occurrence of heat absorption, storage, and release,  
143 and moisture (liquid/vapour) absorption, storage and release (Hall, 2010). In air with a given relative humidity and  
144 temperature, a porous building material, after some period of time exposed to such an environment, will reach a state  
145 of equilibrium with this environment, exchanging the water in its pores with the ambient air. This relationship between  
146 the water content and relative humidity is described by the sorption isotherm (Hansen, 1986). If the equilibrium is  
147 achieved during drying, desorption isotherm is produced, and if achieved during wetting, the sorption isotherm is  
148 realised (BS EN ISO 12571, 2013).

## 149 **3. Material**

150 The WW material used in the experiments was taken from a Welsh saw mill, and was the by-product of furniture and  
151 joinery manufacturing. The material was used as received without addition of binders. The material particle size was  
152 variable but within the range of approximately 1 - 4 mm and in a shape of long and thin curl (Fig.1).



153

154 Fig. 1. Wood waste as received from the saw mill (Source: Plant Fibre Technology ©)

155 WW can be applied to timber frame wall construction in the same way as the current application of cellulose fibres  
156 (CF). CF can either be installed by 'loose fill' or 'wet spray method'. In the loose fill application, CF are first separated

157 by pneumatic equipment, and then are delivered by air pressure into wall cavities through a hose. In the wet spray  
158 application, a separate pump is used to spray water and CF simultaneously in order to increase the adherence of the  
159 fibres (Hurtado *et al.*, 2016). For both applications, when WW is used, it can slump under its own weight creating a  
160 void at the top of the insulated space. The settlement serves to reduce the overall thermal resistance due to increased  
161 heat transfer in the, relatively wide and un-filled, air void (Shea *et al.*, 2013). Generally, for all practical insulation  
162 densities, thermal conductivity increases with increasing density and it is, therefore, important to place WW into the  
163 wall construction at a density that balances adequate thermal resistance against ability to resist slump.

164 The hygroscopic nature of wood permits absorption and desorption of water vapour from the surrounding  
165 environment, tending only to reach an equilibrium condition when the atmospheric relative humidity is stable. Under  
166 varying environmental relative humidity conditions, typical of most occupied buildings, the moisture of wood is  
167 changing continuously and an equilibrium is rarely reached (Popescu and Hill, 2013). Therefore, determining both  
168 the thermal and hygroscopic properties of WW, as a wood residue, will be beneficial in order to facilitate dynamic  
169 simulation of its performance and support design decisions for its use in timber frame wall construction as a thermal  
170 insulation material.

#### 171 **4. Experimental Methods**

172 The experiments conducted to determine the apparent (bulk) density, thermal conductivity, water vapour transmission  
173 properties, true (absolute) density, water absorption coefficient and hygroscopic sorption/desorption properties of  
174 WW are explained in the following sections along with a description of the test equipment, sample preparation, and  
175 test procedures.

##### 176 **4.1. Determination of Apparent (bulk) Density**

177 The apparent (bulk) density of WW was determined in accordance with BS EN 1602 which specifies the equipment  
178 and procedures for determining the apparent density under reference conditions (BSI, 2013a).

##### 179 **Preparing Samples and Test Procedures**

180 Three simple timber frames with the dimension of 400 x 400 mm were constructed and a 400 x 400 OSB sheet with  
181 a thickness of 9 mm was fixed to the frame to form a rigid base to contain the WW material for laboratory testing.  
182 The depths of the frames were 60, 50 and 40 mm in order to produce the samples with different densities, but equal  
183 masses. These depths of containers were selected to suit the value required in the standard for testing loose-fill  
184 materials (BSI, 2001a; ISO 8301), which must be at least 10 times the mean dimension of the beads, grains, flakes,  
185 etc. of the loose-fill material.

186 The WW material was first dried in the oven at 50°C until its mass became constant. The mass was accepted to  
187 become constant when the change of mass between three consecutive weighings became less than 0,1 % of the  
188 total mass according to BS EN ISO 12571 (BSI, 2013c). The oven temperature was lower than prescribed in BS EN  
189 ISO 12570 (BSI, 2013) but was chosen to limit surface scorching of low density WW, which was experienced at

190 higher temperatures. Accordingly, whilst stable mass was attained for all samples it is likely that some moisture may  
191 remain in the material. When the material had attained a constant mass, generally after around 48 hours, the samples  
192 were removed from the oven and placed into a conditioning room at controlled conditions of  $23\pm 3^{\circ}\text{C}$  and relative  
193 humidity of  $50\pm 5\%$ . The time required for the conditioning of the wood waste was between 20 and 25 days. Fig. 2  
194 presents the drying and conditioning facilities used for the WW material.



200 Fig. 2. a) Drying WW, b) Conditioning WW.

201 After conditioning, the WW material was placed into a wood frame with a depth of 60 mm to a density that it would  
202 not slump under its own weight; the resulting mass of this material was measured by an electronic balance with a  
203 maximum capacity of 32 kg and resolution of 1 g. As the material does not have a rigid form, its volume was taken  
204 to be equal to the internal volume of the frame. The apparent density of WW in the frame,  $\rho$ , in  $\text{kg}/\text{m}^3$ , was then  
205 calculated using Equation 1.

$$\rho = m / V \quad \text{(Equation 1)}$$

207 where

208  $m$  is the mass of the test specimen, in kg;

209  $V$  is the volume of the test specimen, in  $\text{m}^3$ .

210 The same mass of material as used in the 60 mm deep container was placed, under compression, into the other  
211 frames which had depths of 50 mm and 40 mm, and the density was then determined using the same approach.

#### 212 4.2. Determination of Thermal Conductivity

213 The thermal conductivity of the WW material was determined in accordance with BS EN 12667 and ISO 8301. BS  
214 EN 12667 specifies principles and testing procedures for determining, by means of the guarded hot plate or heat flow  
215 meter methods, the thermal resistance of test specimens having a thermal resistance of not less than  $0.5 \text{ m}^2\text{-K}/\text{W}$   
216 (BSI, 2001a). ISO 8301 defines the use of the heat flow meter (HFM) method to measure the steady-state heat  
217 transfer through flat slab specimens and the calculation of the heat transfer properties of specimens (ISO, 1991).  
218 Two types of thermal test instruments, ISOMET 2114 (for small samples) and Lasercomp FOX 600 Heat Flow Meter  
219 (for larger sample sizes up to  $600 \times 600 \text{ mm}$ , but not less than  $250 \text{ mm} \times 250 \text{ mm}$ ), were used for thermal conductivity  
220 testing.

221 The Applied Precision ISOMET 2114 is a portable hand-held measuring instrument for direct measurement of thermal  
222 transfer properties of a wide range of isotropic materials including cellular insulating materials, plastics, glasses and

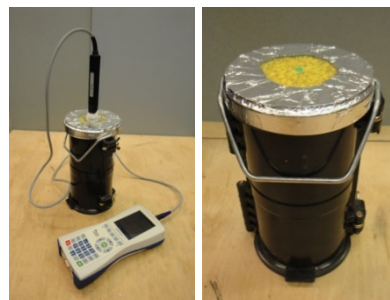


223 minerals. It is equipped with two optional types of measurement probes: needle probes for soft materials and surface  
224 probes for hard materials. The instrument applies a dynamic measurement method, which results in a much reduced  
225 measurement time in comparison with steady state measurement methods. The ISOMET measures the quantities of  
226 thermal conductivity (W/mK), volumetric heat capacity (J/m<sup>3</sup>K), thermal diffusivity (m<sup>2</sup>/s), and temperature (°C) (AP,  
227 2011).

228 The Lasercomp FOX600 is a Heat Flow Meter (HFM) instrument. In a heat flow meter, a specimen is positioned  
229 between two temperature controlled plates. These plates establish a user-defined temperature difference across the  
230 sample (LaserComp, 2010). The sample thickness can be set to match the target thickness of compressible samples,  
231 or, in the case of our test, the actual sample dimension, as detected by four in-built optical encoders. The resulting  
232 heat flux from steady-state heat transfer through the specimen is measured by two proprietary thin film heat flux  
233 transducers covering a large area of upper and lower sample surfaces and the thermal conductivity determined by  
234 reference to a calibration standard.

### 235 **Preparing Samples and Testing Procedure**

236 The tests using the ISOMET 2114 were performed for three different densities determined in Section 4.1, and two  
237 different moisture states, namely, oven-dried and conditioned to 50% RH. The material was placed into a cylindrical  
238 plastic container (Fig. 3). A plastic plate with a hole in the middle was installed over the container, and then the  
239 container was completely sealed with an aluminium foil to limit interaction between room air and the contained  
240 material. The needle probe of the ISOMET was inserted into the material, and the thermal conductivity of the material  
241 was measured.

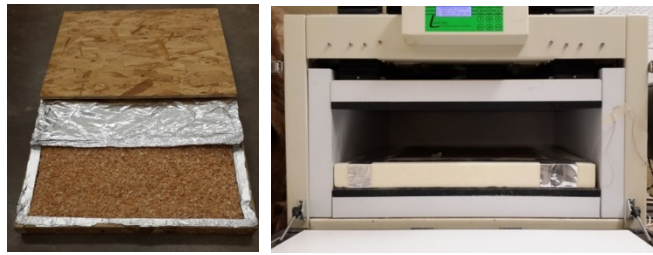


242 Fig. 3. Thermal conductivity testing using the ISOMET 2114 thermal analyser.

### 243 **Heat Flow Meter thermal conductivity measurements**

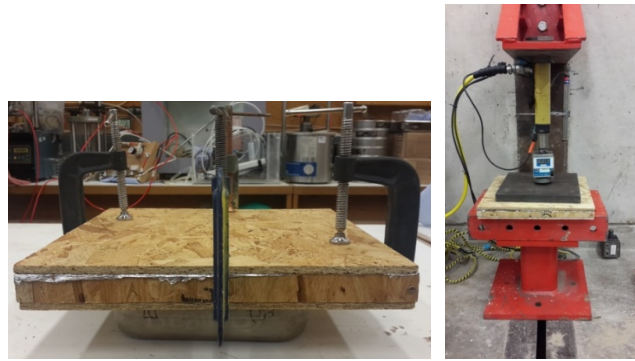
244 Prior to testing in the HFM, the wood frames and the WW were conditioned to the maintained condition of the  
245 University conditioning chamber, as described in Section 4.1. The weights of the WW material and the frames were  
246 measured throughout the conditioning process until they had achieved a constant mass, which was the state that the  
247 change of mass between three consecutive weighings, each made at least 24 h apart, became less than 0,1 % of  
248 the total mass. After drying, the interior surfaces of the frames were lined with an aluminium foil to limit exchange of  
249 moisture between the test material and the frame or external environment, which could affect the thermal  
250 measurements of the WW material. Finally, equal amounts of WW were placed into the wood frames and covered

251 with an OSB sheet and sealed (Fig. 4a). These samples, prior to being placed into the HFM instrument,  
252 surrounded by a thermal insulation board, which was made from polyisocyanurate ( $\lambda = 0.022 \text{ W/mK}$ ), to further limit  
253 edge heat losses (Fig. 4b).



254 (a) (b)  
255 Fig. 4. a) WW and foil-lined OSB frame, b) WW and insulation in the HFM instrument.

256 The WW placed into the frame with the greatest volume (depth equal to 60 mm) was achieved through simple light  
257 compression by hand. However, the same amount of material placed into the frame with the thickness of 50 mm  
258 required compression from a series of G-clamps (Fig. 5a); and for the smallest volume frame (depth equal to 40 mm)  
259 a press was used to apply a pressure of 25 kN (Fig. 5b).



260 (a) (b)  
261 Fig. 5. a) The compression of wood frames by G-clamps, b) heavy-duty press machine.

262 Since the apparent (i.e. measured) thermal conductivity of materials will change depending on their temperatures as  
263 well as their densities and moisture contents, the samples were tested at different temperatures as presented in  
264 Table 1.

265 In a HFM, a temperature gradient is established through closely-controlled heating or cooling of the two plates that  
266 sandwich the test specimen. Within the range for which the HFM is calibrated ( $-15\text{C}$  to  $65\text{C}$ ) and depending on  
267 external cooling capacity, the temperature of each plate and hence heat flow direction can be selected by the user.  
268 In agreement with the recommendations of the relevant test standards, all tests were conducted with an upward heat  
269 flow direction and thus the lower plate was hotter than the upper plate. These tests, similar to the tests performed by  
270 ISOMET, were carried out for two different moisture states, namely, oven-dried and conditioned to 50% RH.

271  
272  
273  
274

275

Table 1. HFM temperature set-points for all specimen samples.

Plate and mean temperatures (Samples 1, 2 and 3)		
T <sub>upper plate</sub> (°C)	T <sub>mean</sub> (°C)	T <sub>lower plate</sub> (°C)
10	20	30
20	30	40
30	40	50

276

277 The raw HFM test results represent the total thermal resistance of both the frames and the WW material, i.e. the  
 278 whole sample, including the OSB and timber frame. The thermal conductivity of the WW material alone was  
 279 determined using Equation 2.

$$280 \quad R_{\text{WHOLE SAMPLE}} = R_{\text{WOOD FRAME}} + R_{\text{WOOD WASTE}}$$

$$281 \quad d_{\text{WS}}/\lambda_{\text{WS}} = d_{\text{WF}}/\lambda_{\text{WF}} + d_{\text{WW}}/\lambda_{\text{WW}} \quad (\text{Equation 2})$$

282 where

283 R : thermal resistance;

284 d : thickness;

285  $d_{\text{WS}}$  : the whole sample;

286  $d_{\text{WF}}$  : the wood frame;

287  $d_{\text{WW}}$  : the wood waste.

288 Equation 2 treats the sample as if formed of three, horizontal, homogeneous layers comprising OSB sheet, WW  
 289 material, OSB sheet. The middle layer of the test sample clearly comprises both a perimeter wood frame and a thin  
 290 vertical OSB edge, however, non-planar heat transfer is assumed to be negligible and is ignored as the area over  
 291 which HFM measurements are recorded (a central thermopile core of approx. 254 mm x 254 mm) is much smaller  
 292 than the area of the test specimen (400 mm x 400 mm), which is further surrounded by rigid insulation as indicated  
 293 in Fig. 4b.

#### 294 4.3. Determination of Hygroscopic Sorption/Desorption Properties

295 The hygroscopic sorption/desorption properties of the wood waste material were determined in accordance with BS  
 296 EN ISO 12571 (BSI, 2013) using the desiccator method with suitable salt solutions to attain the desired range of  
 297 relative humidity.

#### 298 Preparing Samples and Testing Procedure

299 Three samples with the dimensions of 100 mm x100 mm were prepared. The samples of oven-dried WW were  
 300 contained in a plastic mesh to achieve a density of 117 kg/m<sup>3</sup> (Fig. 6a). The open mesh of the container allowed the  
 301 WW to exchange moisture with the conditioned air in the desiccator chamber until equilibrium with the environment  
 302 was attained. Table 2 presents the relative humidity values selected for measuring sorption/desorption at the air  
 303 temperature of 23°C and the required salt solutions.

304

Table 2. Relative humidity and salt solutions.

No	Salt	Relative Humidity (%)
1	MgCl <sub>2</sub> .6H <sub>2</sub> O	33
2	Mg(NO <sub>3</sub> ) <sub>2</sub> .6H <sub>2</sub> O	53
3	NaCl	75
4	KNO <sub>3</sub>	93

306

307 The sorption test was initiated with the solution prepared by mixing MgCl<sub>2</sub>.6.H<sub>2</sub>O and distilled water. This solution  
 308 was put into a glass plate first, and then this plate was placed to the container to maintain the required relative  
 309 humidity. A metal mesh was installed at 5 cm above the plate to raise the samples above the fluid level. A thin  
 310 watertight, but vapour permeable, insulation layer was placed on the mesh to protect the samples from the solution.  
 311 Prior to placing the samples in the desiccator, the mass of each sample was measured. After placing the samples,  
 312 all joints between the container and its cover were sealed with an aluminium tape (Fig. 6b). Finally, the entire  
 313 container was placed in a conditioning room which maintained an air temperature of (23±0.5)°C and a relative  
 314 humidity of (50±5)%. The mass of the samples was periodically measured until they were in equilibrium with the  
 315 environment (constant mass), which was the state that the change of mass between three consecutive weighings  
 316 became less than 0,1 % of the total mass. When the aluminium tape was opened to measure the weight of the  
 317 samples during the test, the relative humidity and the temperature inside the container were also checked with a  
 318 humidity- temperature meter. This checking procedure can be seen in Fig. 6c. The measurements showed that the  
 319 salt solutions provided the target conditions. After reaching the equilibrium, the test was repeated with  
 320 Mg(NO<sub>3</sub>)<sub>2</sub>.6H<sub>2</sub>O, NaCl, and KNO<sub>3</sub> respectively.

321

322

323

324

325



326

327

Fig. 6. a) The samples, b) The test set-up for desiccator method,  
 c) The humidity / temperature meter inside the container.

328 The desorption test began with the solution of KNO<sub>3</sub> and distilled water, and the test was then repeated with NaCl,  
 329 Mg(NO<sub>3</sub>)<sub>2</sub>.6H<sub>2</sub>O, and MgCl<sub>2</sub>.6.H<sub>2</sub>O respectively.

#### 330 4.4. Determination of Water Vapour Transmission Properties

331 The water vapour transmission properties of WW were determined in accordance with BS EN ISO 12572 which  
 332 specifies a method based on cup tests for determining the water vapour permeance of building products and the  
 333 water vapour permeability of building materials under isothermal conditions (BSI, 2001b).

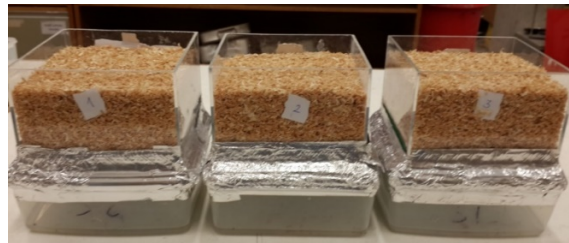
## 334 Preparing Samples and Testing Procedure

335 Tests were conducted for both 'dry and wet cup' states, which provided information about the performance of the  
336 WW material under low and high humidity conditions respectively. The accepted test conditions according to BS EN  
337 ISO 12572 are presented in Table 3.

338 Table 3. Water vapour transmission test conditions.

Set	Condition (°C - RH%)	Tolerances		
		Temperature (°C)	Relative humidity (RH, %)	
			Set point	Tolerance
Dry State	23 - 50	23 ± 0,5	0	+3
Wet State	23 - 50	23 ± 0,5	93	±3

339  
340 Three plastic containers with length and width each of 150 mm and a height of 80 mm were cut, leaving the upper  
341 and bottom surfaces open. The bottom surfaces of these containers were covered with a plastic mesh, and filled with  
342 the conditioned WW, to a density of 117 kg/m<sup>3</sup>. Every sample was then placed over the mouth of a test cup having  
343 approximately the same size aperture as the plastic container, which included silica gel for the dry cup test. The joints  
344 between the containers and the test cup were sealed with an aluminium tape. Finally, the test samples were placed  
345 into the conditioning room. The weights of the samples were periodically measured to determine the rate of water  
346 vapour transmission in the steady state; the containers remained sealed for the duration of the test. For the wet cup  
347 test, the samples were prepared in the same manner as for the dry cup test but with Potassium nitrate (KNO<sub>3</sub>) solution  
348 to provide a relative humidity of 93% (Fig 7).



349  
350 Fig. 7. The samples during the wet cup test.

## 351 4.5. Determination of True (Absolute) Density and Porosity

352 The true density of WW is determined by helium pycnometer, which gives the closest approximation to the true  
353 density of a material. In this method, the helium penetrates the smallest pores, approaching the real volume (Donato  
354 and Lazzara, 2012) and this value was then used to calculate the porosity value of WW.

355 An AccuPyc 1330 gas displacement pycnometer was used during the tests. In our tests, helium gas was used to  
356 provide rapid and accurate results. The test procedure with regards to number of purges, purge fill pressure, number  
357 of runs, and equilibration rate is presented in Table 4.

358

359

360

Table 4. The parameters for the true density tests

Parameters	Data
Number of purges	10
Purge fill pressure	19500 psig
Number of runs	10
Equilibration rate	0.0050 psi/min

361

362 The test set-up comprised of the pycnometer device and the cylinder containing helium as shown in Fig. 8.



363

364

Fig. 8. The test set-up for determining true density.

365 The porosity value of WW is calculated by Equation 3:

366

$$P = 100 \times (1 - (d_b / d_t)) \quad \text{(Equation 3)}$$

367 where

368  $d_b$  : Bulk density

369  $d_t$  : True density

370

### 371 Preparing Samples and Testing Procedure

372 The oven-dried WW was used for this test to prevent the distorting effect of water vapour on the volume measurement. An empty sample cup was first measured, and then the dried material was placed into the cup (Fig. 9). The amount of this material was calculated for the density of 117 kg/m<sup>3</sup>. The sample was then inserted into the cell chamber of the pycnometer device. After modifying the test parameters, the test was initiated. The value of the true density was obtained at the end of 10 purges and 10 runs. The test was repeated three times, and then the mean value of three measurements was calculated.

378

379



Fig. 9. a) The cup including WW b) The cup inserted into the cell chamber.

#### 380 4.6. Determination of Water Absorption Coefficient

381 The water absorption coefficient of WW was determined in accordance with BS EN ISO 15148 which specifies a  
382 method for determining, by partial immersion with no temperature gradient, the short-term liquid water absorption  
383 coefficient (BSI, 2002). Since there is no other standard for loose materials, this method was applied for determining  
384 the water absorption coefficient of WW.

#### 385 Preparing Samples and Testing Procedure

386 The test conditions given in Table 5 were adjusted in accordance with BS EN ISO 15148.

387 Table 5. The water absorption test conditions.

Temperature (°C)	Relative humidity (%)
20 - 26	40 - 60

388  
389 In accordance with the standard, and because of the difficulty in sealing a low density loose fill material, the WW was  
390 placed into a tightly-fitting tube supported on a wire mesh placed over the mouth of the tube. In this test, six plastic  
391 tubes with a diameter of 100 mm and a length of 80 mm were cut from a plastic pipe. The bottom surfaces of these  
392 tubes were covered with a plastic mesh with very small holes (approximately 2 mm in diameter) that prevented the  
393 particles from falling into the water. The containers were filled with the conditioned WW, to a density of 117 kg/m<sup>3</sup>. A  
394 metal grid was then placed into a larger plastic container filled with water. This grid allowed the bases of the samples  
395 remain clear of the bottom of the container. The level of the water in the container was controlled during the test to  
396 ensure that it remained at 5 mm ( $\pm$  2 mm) above the bases of the samples. Finally, six samples were placed over the  
397 grid, and a timer was used to record the partial immersion time. After approximately 5 minutes the samples were  
398 removed from the water, the surfaces were blotted with a damp sponge, and weighed. This procedure including  
399 immersion, removal, surface drying and weighing was repeated at durations of 20 min, 1 h, 2 h, 4 h, 8 h, 12 h, 21 h  
400 and 24 h to provide a series of masses  $m_t$  at times  $t$ . The procedures of blotting and weighing were carried out within  
401 a minute and then the samples were returned to the water immediately afterwards. Fig. 10 presents the test set-up  
402 including the container, grid, samples, scale, timers and sponge.



403

404

Fig. 10. The test set-up for the water absorption test.

405 This test was repeated for the WW sample with a density of 158 kg/m<sup>3</sup> in order to examine the effect of density on  
406 the water absorption of WW.

407 **5. Experimental Results and Discussions**

408 The results of the experiments carried out for determining apparent density, thermal conductivity, hygroscopic  
 409 sorption/desorption curves, water vapour diffusion resistance factor, true density and water absorption coefficient are  
 410 presented in this section.

411 **5.1. Apparent Density**

412 The apparent densities of three samples prepared with the conditioned WW were calculated using Equation 1, as  
 413 described in Section 4.1. The first one, 117 kg/m<sup>3</sup>, is the density at which the WW would resist slump under its own  
 414 weight. The others, 158 kg/m<sup>3</sup> and 167 kg/m<sup>3</sup>, are the resultant values after compression in to shallower containers.  
 415 All results are presented in Table 6. As required and expected, the density of WW increased as the thickness of the  
 416 frame decreased since the cavities in the frame reduced due to the increased compression of the (same mass of)  
 417 material.

418 Table 6. The apparent densities of WW in the different wood frames.

Samples	Density ( $\rho$ - kg/m <sup>3</sup> )
Sample 1 (d= 60mm)	117
Sample 2 (d= 50mm)	158
Sample 3 (d= 40mm)	167
d : thickness of the sample	

419

420 **5.2. Thermal Conductivity**

421 The thermal properties i.e. thermal conductivity, volumetric heat capacity, and thermal diffusivity, measured by the  
 422 ISOMET dynamic thermal analyser for different densities are given in Table 7. The results are presented for both the  
 423 oven-dried WW and the conditioned WW.

424 Table 7. The thermal properties measured for the different densities of WW by ISOMET.

MATERIAL	Density ( $\rho$ - kg/m <sup>3</sup> )	Thermal Conductivity ( $\lambda$ - W/mK)	Volumetric Heat Capacity (VHC - 10 <sup>6</sup> J/m <sup>3</sup> K)	Thermal Diffusivity ( $a$ - 10 <sup>-6</sup> m <sup>2</sup> /s)
Oven-Dried Material	117	0.0528	0.1026	0.5153
	158	0.0554	0.1830	0.3080
	167	0.0558	0.1760	0.3168
Conditioned Material	117	0.0568	0.1546	0.3674
	158	0.0622	0.2249	0.2765
	167	0.0629	0.2133	0.2951

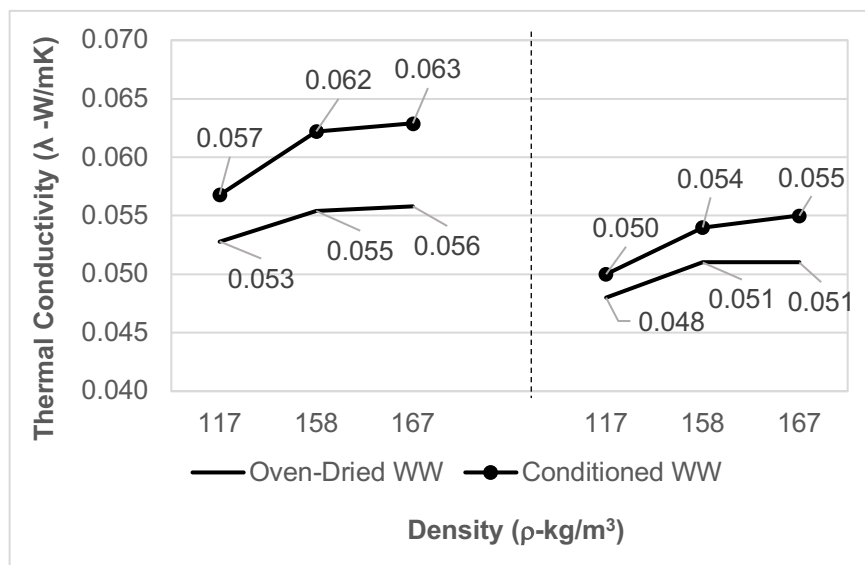
425

426 Fig. 11 presents the thermal conductivity values of WW measured by both the ISOMET device and the Heat Flow  
 427 Meter. The HFM results are presented for the case of a 20°C temperature difference between measurement plates



428 and a mean temperature of 30°C. The values measured by HFM were consistently lower than the values measured  
 429 by the ISOMET unit. The ISOMET applies a dynamic heat flux measurement method, which enables it to reduce the  
 430 measurement time in comparison with steady state measurement methods. The HFM use a steady-state heat flux  
 431 measurement method as explained in Section 4.2. The stated accuracy of the two devices is 1% for the Heat Flow  
 432 Meter (LaserComp, 2010) and 5% of reading+0.001 W/mK for the ISOMET device (AP, 2011). The results taken  
 433 from both instruments, as expected, indicated that the increased moisture content due to conditioning of the material  
 434 caused the thermal conductivity to increase.

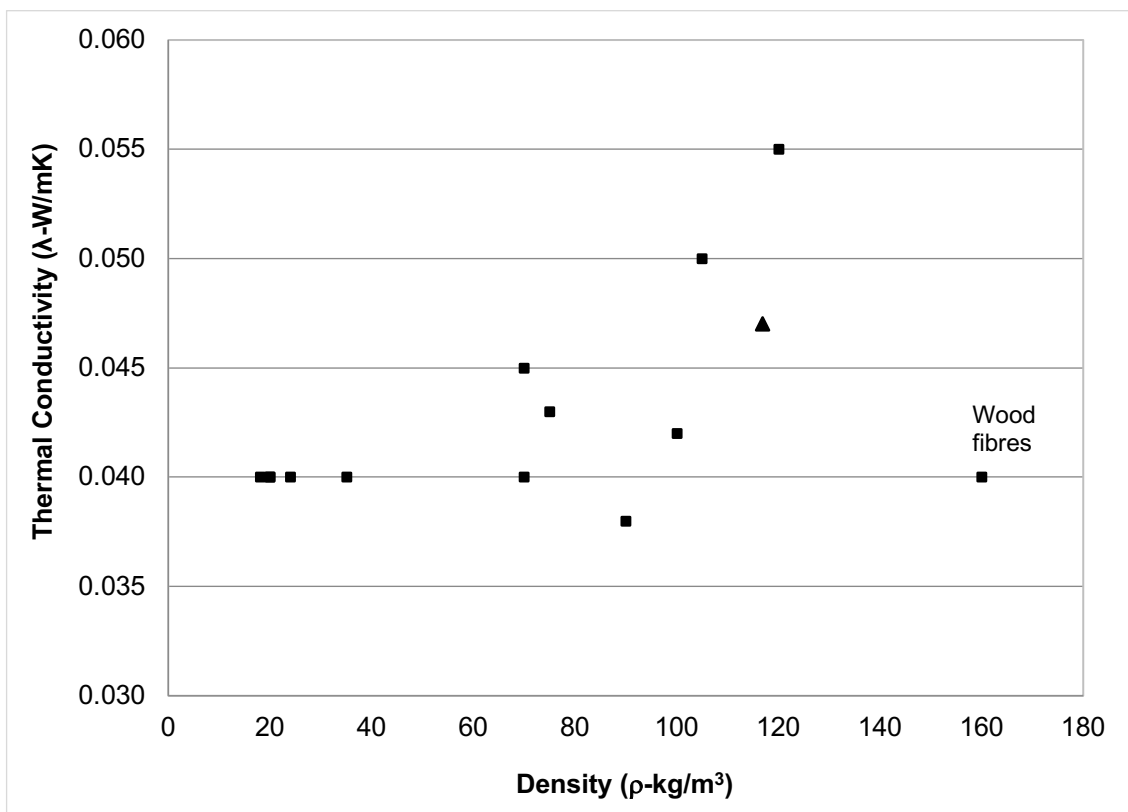
435 Whilst the expected general trend of increasing apparent thermal conductivity with increasing density, increasing  
 436 moisture content, and increasing temperature is apparent (Figures 11 and 13), it is evident that, accepting the  
 437 different degree of error between the HFM and ISOMET devices, there is a consistently higher value of thermal  
 438 conductivity reported by the ISOMET device (Figure 11) relative to the HFM; the difference between the apparent  
 439 thermal conductivity being greatest for the conditioned samples. The transient measurement method employed by  
 440 the ISOMET needle probe, a variation of the Hot Wire method, has some advantages relative to the Heat Flow Meter  
 441 e.g. reduced sample material quantity, small temperature gradient, and short test duration. However, other  
 442 investigators (Campanale and Moro, 2016) have identified that the heating sensor causes a latent heat exchange  
 443 due to the phase changes in the water inside the specimen close to the sensor, and this influences the thermal  
 444 conductivity measured value. Whilst the Heat Flow Meter causes moisture migration between hot and cold plates it  
 445 has been demonstrated (Deganello et al., 2013, cited in Campanale and Moro, 2016) that for specimens with a  
 446 moisture content lower than 8.5% the error due to phase changes and moisture redistribution is less than 2.5% if the  
 447 thermal conductivity is derived from the HFM measurements recorded after reaching steady state, which is the case  
 448 for our presented results.



449 Fig. 11. The thermal conductivity values for different densities of WW by HFM and ISOMET.

451

452 In addition to variations due to moisture, density and temperature, there are numerous other factors that could  
 453 influence the measured thermal conductivity in both test methods including, for example, surface contact resistance,  
 454 inhomogeneity in the material sample, sample geometry, directional-dependencies (anisotropy) etc. For the oven  
 455 dried samples, the difference between HFM and the ISOMET device is +/-10%. Rides et al. (2009) performed inter-  
 456 comparison tests of a range of methods including both Hot Wire probes and Heat Flow Meters and observed  
 457 variations of 6% for thermal conductivity, albeit on a more homogeneous and isotropic plastic material.  
 458 The measured thermal conductivity of oven-dried value of WW (0.048 W/mK) with the density of 117 kg/m<sup>3</sup> is similar  
 459 to that of the lower density wood chipping material reported in Gellert (2010); and better than cereal and reeds of  
 460 similar density (Fig. 12).



475 Fig. 12. Thermal conductivity versus density for different natural insulation materials

476  
 477 Fig.13 presents the temperature-dependent thermal conductivity, as measured using the HFM, of the oven-dried and  
 478 conditioned WW for all densities.

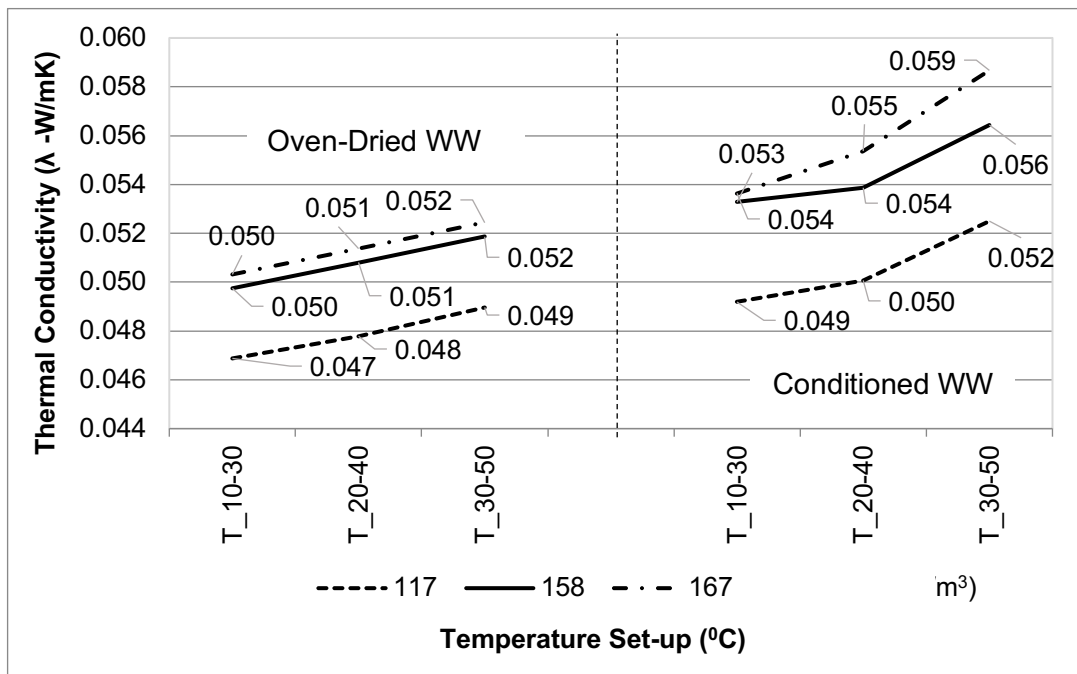


Fig. 13. Thermal conductivity values measured by HFM for WW.

479

480

481 As expected, the thermal conductivity of the material increased as the temperature increased for both the oven-dried  
 482 and conditioned WW, and all densities. The thermal conductivity of the conditioned samples was higher due to their  
 483 increased moisture contents. While the differences between the oven-dried and conditioned samples changed  
 484 7-11% when measured by ISOMET, they changed 4-7% when measured by HFM because of the different  
 485 measurement methods of the devices as discussed in Section 5.2.

486 **5.3. Determination of Hygroscopic Sorption/Desorption Properties**

487 The moisture contents at each relative humidity were calculated using Equation 4 as presented in BS EN ISO 12571  
 488 (BSI, 2013). These values and their standard deviations for each relative humidity are given in Table 8. According to  
 489 the results, the biggest difference in the moisture contents of the samples were calculated for 93% RH during the  
 490 sorption.

491 
$$u = (m - m_0) / m_0 \quad \text{(Equation 4)}$$

492 where

493  $m$  : the mass of the test specimen at each relative humidity.

494  $m_0$  : the initial mass of the test specimen

495 Table 8 The moisture contents at each relative humidity.

Samples	Moisture contents at sorption				Moisture contents at desorption			
	33%RH	53%RH	75%RH	93%RH	93%RH	75%RH	53%RH	33%RH
Sample 1	0,045	0,068	0,109	0,153	0,159	0,118	0,086	0,069
Sample 2	0,045	0,065	0,106	0,143	0,159	0,123	0,082	0,072
Sample 3	0,044	0,067	0,109	0,149	0,158	0,116	0,082	0,067
St Deviations	0,0005	0,0017	0,0019	0,0050	0,0005	0,0036	0,0023	0,0024

496

497

498 The moisture contents of WW versus the relative humidities inside the plastic container during the test are given in  
 499 Fig. 14. In common with isotherm test results for many other materials, hysteresis was observed in the material. The  
 500 duration of the tests varied between 20 and 30 days depending on the target relative humidity. It took approximately  
 501 one month for the high relative humidity values to be obtained. The moisture content of WW from 33%RH and 93%RH  
 502 increased approximately 11% at sorption, and decreased approximately 9% during desorption across the same  
 503 range. In addition, the moisture content increased more rapidly from 53%RH upwards.

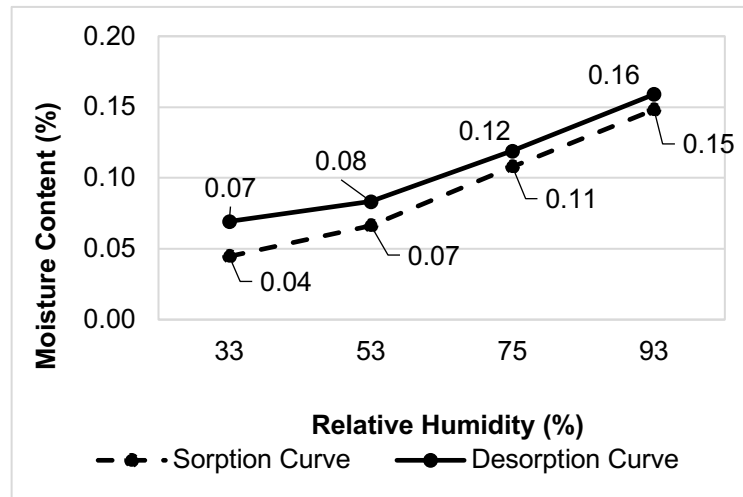


Fig. 14. Sorption and desorption curves for WW.

504

505

506

507 **5.4. Determination of Water Vapour Transmission Properties**

508 Table 9 presents the results of the dry and wet cup tests for WW calculated using Equations 5-10, and the standard  
 509 deviation values calculated for three samples. As expected, these results indicate that WW has a low water vapour  
 510 resistance at high relative humidity compared to the low relative humidity conditions. Moreover, the permeability of  
 511 WW was higher at high relative humidity, i.e. the permeability of the material increased as the relative humidity  
 512 increased.

513

514

515

516

517

518

519

520

Table 9. The results of the dry and wet-cup tests for WW.

Water Vapour Transmission Properties	Eq (5-10)	Dry Cup Test	Standard Deviation (three samples)	Wet Cup Test	Standard Deviation (three samples)
Water Vapour Permeability ( $\delta$ ) - (kg/msPa)	$\delta = W.d$ (Eq.5)	2.20E-11	4,27E-13	4.92E-11	1,07E-12
Water Vapour Diffusion Resistance Factor ( $\mu$ ) - (-)	$\mu = \delta_{air}/\delta$ (Eq.6)	9,06	1,76E-01	4,05	8,92E-02
Water Vapour Diffusion Equivalent Air Layer Thickness ( $s_d$ ) - (m)	$s_d = \mu.d$ (Eq.7)	0.68	1,32E-02	0.30	6,69E-03
Water Vapour Transmission Rate ( $g$ ) - (kg/m <sup>2</sup> s)	$g = G/A$ (Eq.8)	4.19E-07	8,16E-09	9.39E-07	2,05E-08
Water Vapour Permeance ( $W$ )- (kg/m <sup>2</sup> sPa)	$W = G/A. \Delta p_v$ (Eq.9)	2.93E-10	5,70E-12	6.56E-10	1,43E-11
Water Vapour Resistance ( $Z$ ) - (m <sup>2</sup> sPa/kg)	$Z = 1/W$ (Eq.10)	3.42E+09	6,65E+07	1.53E+09	3,31E+07
<p><u>Other Abbreviations</u>  <math>d</math> : Layer thickness  <math>s_d</math> : Water Vapour Diffusion Equivalent Air Layer Thickness  <math>G</math> : Water vapour flow rate through specimen  <math>\Delta p_v</math> : Water vapour pressure difference across specimen  <math>A</math> : Area of specimen  Eq : Equation</p>					

522

523

The results of the dry and wet cup tests conducted by Vololonirina *et al.* (2014) for wood fibre (WF) material are

524

compared to our results for wood waste (WW) in Table 10.

525

Table 10. The results of the dry and wet-cup tests for WW and WF.

	Dry Cup Test		Wet Cup Test	
	WF	WW	WF	WW
Water Vapour Permeability ( $\delta$ ) - (kg/msPa)	3.60E-11	2.20E-11	8.30E-11	4.92E-11
Water Vapour Diffusion Resistance Factor ( $\mu$ ) - (-)	6	9.06	2	4.05

526

527

The cup tests demonstrate that WW has slightly increased resistance to water vapour diffusion relative to the WF

528

material; proportionally more so at the higher humidities of the Wet Cup test where the transport of liquid water

529

increases and vapour transport diminishes. Where transfer is dominated by vapour diffusion, WW records diffusion

530

resistance more than 50% higher than WF.

531

532 **5.5. Determination of True (Absolute) Density and Porosity**

533 The true density values measured by the Pycnometer device and the porosity (P, %) values calculated by Equation  
 534 3 for the density of 117 kg/m<sup>3</sup> of are presented in Table 11. Since the true density measurements repeated three  
 535 times gave similar results to each other without obtaining any extreme value, their means were given in the table.

536 Table 11. The measured true densities and the calculated porosity values for different densities.

Apparent (Bulk) Density (g/cm <sup>3</sup> )	True (Absolute) Density (g/cm <sup>3</sup> )	Porosity (%)
0.117	4.348*	97
* The mean value of three measurements.		

537  
 538 The porosity results revealed that WW is comparable to other natural fibre materials such as those recorded by  
 539 Palumbo *et al.* (2016) which included hemp fibre, wood wool and wood fibre which were 97%, 96% and 86%,  
 540 respectively.

541 **5.6. Determination of Water Absorption Coefficient**

542 The mean mass change of six samples, and for two densities, versus the square root of the weighing times, is  
 543 presented in Fig. 15. The difference between the mass at each weighing and the initial mass were divided by the  
 544 area of the open end of the sample (Equation 11), and plotted against the square root of the weighing times,  $\sqrt{t}$ .

545 
$$\Delta m_t = (m_t - m_i) / A \quad \text{(Equation 11)}$$

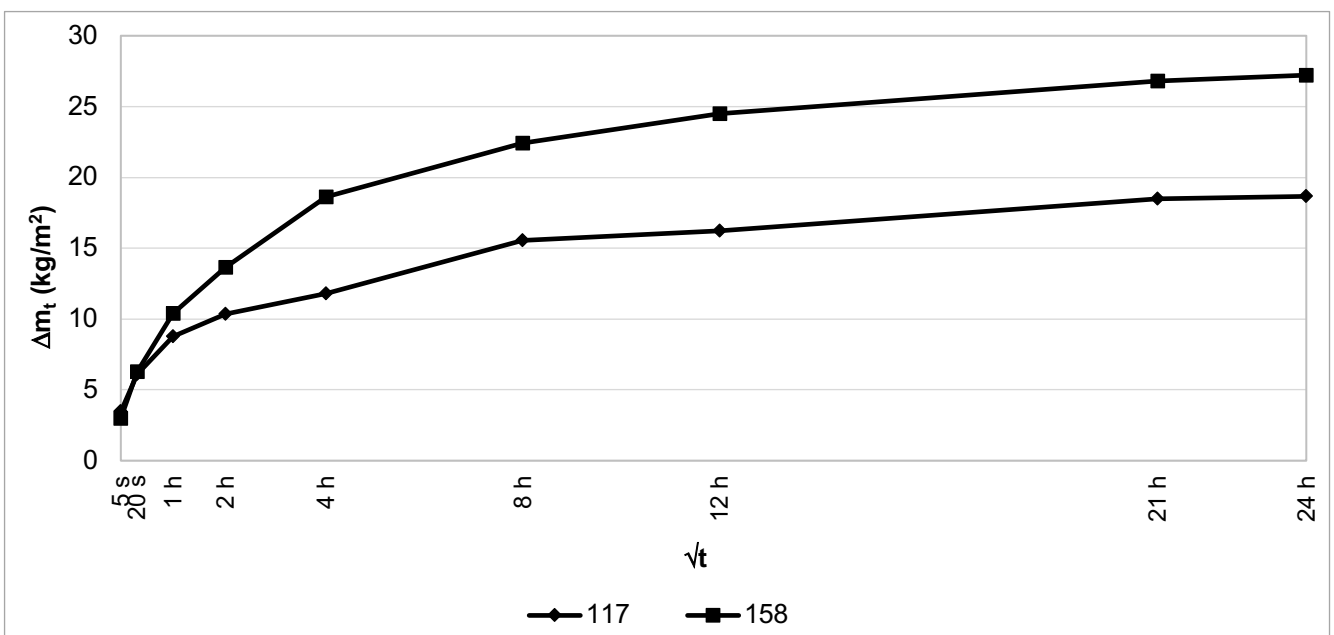
546 where

547  $m_t$  mass of sample 24 h after the start of the test;

548  $m_i$  initial mass of sample;

549 A area of open end of sample;

550 t time.



551  
 552 Fig. 15. The mass changes versus weighing times for two densities.

553 The water absorption coefficients for two densities were calculated according to BS EN ISO 15148 (BSI, 2002) by  
554 using Equation 12, and the results were given in Table 12.

555 
$$A_{w24} = m_{tf} / \sqrt{86400}$$
 Equation (12)

556 where

557  $m_{tf}$  : the value of  $m$  24 h after the start of the test

558

559 Although limited to sample of just two different densities, the water absorption coefficient increases as the density  
560 increases. The samples with the density of 158 kg/m<sup>3</sup> absorbed the water approximately 48% more than the ones  
561 with the density of 117 kg/m<sup>3</sup> due to increasing the amount of particles.

562 Table 12. The water absorption coefficients for different densities

Density ( $\rho$ - kg/m <sup>3</sup> )	Water absorption coefficient ( $A$ - kg/m <sup>2</sup> s <sup>0.5</sup> )
117	0,063
158	0,093

563

564 According to Mukhopadhyaya *et al.* (2002) white pine wood, red clay brick and concrete have water absorption  
565 coefficients of 0.0112 kg/m<sup>2</sup>s<sup>0.5</sup>, 0.084 kg/m<sup>2</sup>s<sup>0.5</sup> and 0.184 kg/m<sup>2</sup>s<sup>0.5</sup>, respectively, at a temperature of 21°C. When  
566 these values are compared to our results, it is seen that WW's water absorption coefficient is very close to red clay  
567 brick's.

## 568 6. Conclusions

569 Current insulation materials used in construction industry are generally inorganic based materials such as extruded  
570 polystyrene, expanded polystyrene, and polyurethane foam. Although these materials have a high performance with  
571 regards to the resistance to conduction heat transfer, their environmental impacts during the building life cycle period,  
572 and especially in the production process, are generally high. Therefore, the use of bio-based materials instead of  
573 inorganic based materials has become an important issue in terms of reducing environmental impacts and improving  
574 building whole life cycle performance primarily with regards to reduced embodied energy.

575 For this research, the characterisation of the hygrothermal properties of waste wood (WW) was undertaken with the  
576 aim to provide greater understanding of the material performance and its application as an insulation material in  
577 timber frame wall construction.

578 WW can be applied to timber frame wall construction by manual filling or mechanical blowing of the loose fill material  
579 between the studs of the frame and without any binder. The density of 117 kg/m<sup>3</sup> was found to be a functional density  
580 level that can be achieved without mechanical compression and has thermal performance comparable to similar  
581 materials. However, its suitability at full-scale requires further investigation to ensure that the material does not slump  
582 under its own weight, which would lead to overall increased heat loss. According to the experimental results obtained

583 in this investigation, WWV could be efficiently used as a thermal insulation material. Its measured thermal conductivity  
584 value was close to the values of wood fibres, wood chippings and straw bale, and lower than reeds and cereal, which  
585 have already been used as natural insulation materials in the construction market. When compared to inorganic  
586 insulation materials, it has a higher thermal conductivity value. The moisture content at a range of relative humidities  
587 during sorption and desorption testing was similar to reported values for wood fibre material. Additionally, we have  
588 reported a range of hygric and thermal material properties at a range of densities, which can be used to facilitate  
589 Hygrothermal analysis, e.g. through computer simulation with tools such as WUFI, which can in-turn provide valuable  
590 supporting information for evaluation of low impact building designs employing this natural low cost and low impact  
591 locally available material.

## 592 **Acknowledgement**

593 This research was funded by the Scientific and Technical Research Council of Turkey (TUBITAK) within the frame  
594 of 2219 - International Post-Doctoral Research Fellowship Programme. The authors gratefully acknowledge  
595 TUBITAK for the financial support of this work. The authors also wish to thank Plant Fibre Technology for the supply  
596 of the Wood Waste material and the staff and students of the BRE CICM research group in the Department of  
597 Architecture and Civil Engineering at the University of Bath for their help in the experimental aspects of the work,  
598 particularly PhD student Miss Shaghayegh Mohammad for her assistance in preparation of test specimens.

## 599 **References**

- 600 ▪ Alf-Cemind (2017). Technology Guide - Supporting the use of Alternative Fuels in Cement Industry. [http://www.alf-](http://www.alf-cemind.com/cd/AF_and_ARM_wood_waste.htm)  
601 [cemind.com/cd/AF\\_and\\_ARM\\_wood\\_waste.htm](http://www.alf-cemind.com/cd/AF_and_ARM_wood_waste.htm).
- 602 ▪ AP (2011). ISOMET 2114 Product Catalogue, ISOMET-PC201510-EN, Applied Precision (AP) Ltd.  
603 <http://www.appliedp.com/en/isomet.htm>.
- 604 ▪ Briga-Sa, A., Nascimento, D., Teixeira, N., Pinto, J., Caldeira, F., Varum, H., Paiva, A. (2013). Textile waste as  
605 an alternative thermal insulation building material solution, *Construction and Building Materials* 38, pp.155–160.
- 606 ▪ BSI (2001a). BS 12667 Thermal performance of building materials and products — Determination of thermal  
607 resistance by means of guarded hot plate and heat flow meter methods — Products of high and medium thermal  
608 resistance. The British Standard.
- 609 ▪ BSI (2001b). BS EN ISO 12572 Hygrothermal performance of building materials and products — Determination  
610 of water vapour transmission properties. The British Standard.
- 611 ▪ BSI (2002). BS EN ISO 15148 Hygrothermal performance of building materials and products — Determination of  
612 water absorption coefficient by partial immersion. The British Standard.
- 613 ▪ BSI (2013a). BS EN 1602 Thermal insulating products for building applications. Determination of the apparent  
614 density. The British Standard.



- 615     ▪ BSI (2013b). BS EN ISO 12570:2000+A1:2013 Hygrothermal performance of building materials and products —  
616     Determination of moisture content by drying at elevated temperature. The British Standard.
- 617     ▪ BSI (2013c). BS EN ISO 12571 Hygrothermal performance of building materials and products — Determination  
618     of hygroscopic sorption properties. The British Standard.
- 619     ▪ Campanale, M., Moro, L. (2016). Thermal conductivity of moist autoclaved aerated concrete: experimental  
620     comparison between heat flow method (HFM) and transient plane source technique (TPS), *Transp. Porous Med.*,  
621     113, pp.345-355.
- 622     ▪ Charca, S., Noel, J., Andia, D., Flores, J., Guzman, A., Renteros, C., Tumialan, J. (2015). Assessment of Ichu  
623     fibers as non-expensive thermal insulation system for the Andean regions, *Energy and Buildings* 108, pp.55–60.
- 624     ▪ DEFRA (2013). Wood Waste Landfill Restrictions in England: Call for Evidence Analysis, Department of  
625     Environment Food and Rural Affairs.
- 626     ▪ Deganello, M., Campanale, M., Moro, L. (2013). Effect of moisture movement on tested thermal conductivity of  
627     moist aerated autoclaved concrete, *Transp. Porous Media* 98, pp.125-146.
- 628     ▪ Donato, I.D., Lazzara, G. (2012). Porosity determination with helium pycnometry as a method to characterize  
629     waterlogged woods and the efficacy of the conservation treatments, *Archaeometry* (54), pp.906–915.
- 630     ▪ EPA (1996). Wood Products in the Waste Stream Characterization and Combustion Emissions, Vol. 1, Technical  
631     Report, U.S. Environmental Protection Agency.
- 632     ▪ Gellert, R. (2010). Materials for energy efficiency and thermal comfort in buildings, Part 2- Chapter: 9 Natural fibre  
633     and fibre composite materials for insulation in buildings, Edited by Matthew R. Hall, Woodhead Publishing Limited,  
634     pp.229-256.
- 635     ▪ GUTEX (2015). 'Environmental Product Declaration'. Declaration number: EPD-GTX-20140222-IBC2-EN, Institut  
636     Bauen und Umwelt e.V. (IBU).
- 637     ▪ Hall, M.R. (2010). Materials for energy efficiency and thermal comfort in buildings, Part 2-Chapter 14:  
638     Hygrothermal materials for heat and moisture control in buildings, Edited by Matthew R. Hall, Woodhead  
639     Publishing Limited, pp.345-364.
- 640     ▪ Hansen, K.K., Sorption Isotherms - A catalogue, Technical Report 162/86, Building Materials Laboratory, The  
641     Technical University of Denmark, December 1986.
- 642     ▪ HPBP (2014). Intro to GUTEX Wood Fiber Board: vapor open continuous insulation & WRB', 475 High  
643     Performance Building Supply, [https://www.foursevenfive.ca/the-gutex-wood-fiber-board-primer-vapor-open-](https://www.foursevenfive.ca/the-gutex-wood-fiber-board-primer-vapor-open-continuous-insulation-wrb/)  
644     [continuous-insulation-wrb/](https://www.foursevenfive.ca/the-gutex-wood-fiber-board-primer-vapor-open-continuous-insulation-wrb/)
- 645     ▪ Hurtado, P.L., Rouilly, A., Vandebossche, V., Raynaud, C. (2016). A review on the properties of cellulose fibre  
646     insulation, *Building and Environment* 96, pp.170-177.

- 647   ▪ ISO 8301 (1991). Thermal insulation — Determination of steady-state thermal resistance and related properties  
648   — Heat flow meter apparatus.
- 649   ▪ Korjenic, A., Teblich, L., Bednar, T. (2010). Increasing the indoor humidity levels in buildings with ventilation  
650   systems: simulation aided design in case of passive houses, *Building Simulation* 3 (7), pp.295–310.
- 651   ▪ Korjenic, A., Petranek, V., Zach, J., Hroudova, J. (2011). Development and performance evaluation of natural  
652   thermal-insulation materials composed of renewable resource, *Energy and Buildings* 43, pp.2518–2523.
- 653   ▪ LaserComp (2010), FOX600 and FOX800 Series Instruments Manual, U.S.A.
- 654   ▪ Lawrence, M., Shea, A., Walker, P. and De Wilde, P. (2013). Hygrothermal performance of bio-based insulation  
655   materials. *Proceedings of the Institution of Civil Engineers: Construction Materials*, 166 (4), pp.257-263.
- 656   ▪ Mukhopadhyaya, P., Kumaran, K., Normandin, N., Goudreau, P. (2002). Effect of surface temperature on water  
657   absorption coefficient of building materials, NRCC-45369, IRC, Canada.
- 658   ▪ Moon, H.J, Ryu, S.H., Kim, J.T. (2014). The effect of moisture transportation on energy efficiency and IAQ  
659   inresidential buildings, *Energy and Buildings*, 75, pp.439–446.
- 660   ▪ Osanyintola, O.F., Simonson, C.J. (2006). Moisture buffering capacity of hygroscopic building materials:  
661   experimental facilities and energy impact, *Energy and Building* 38, pp.1270–1282.
- 662   ▪ Pacheco-Torgal, F., Jalali, S., Fucic, A. (2012). *Toxicity of Building Materials*, Woodhead Publishing Limited.
- 663   ▪ Palumbo, M., Lacasta, A.M., Holcroft, N., Shea, A., Walker, P. (2016). Determination of hygrothermal parameters  
664   of experimental and commercial bio-based insulation materials, *Construction and Building Materials* (124),  
665   pp.269–275.
- 666   ▪ Panyakaew, S., Fotios, S. (2011). New thermal insulation boards made from coconut husk and bagasse, *Energy  
667   and Buildings* 43, pp.1732–1739.
- 668   ▪ Popescu, C-M., Hill, C.A.S. (2013). The water vapour adsorption-desorption behaviour of naturally aged *Tilia  
669   cordata* Mill. *Wood, Polymer Degradation and Stability* 98, pp. 1804-1813.
- 670   ▪ Rides M., Morikawa J., Halldahl L., Hay B., Lobo H., Dawson A. & Allen C. (2009). Inter comparison of thermal  
671   conductivity and thermal diffusivity methods for plastics, *Polymer Testing*, Vol.28, pp. 480-489.
- 672   ▪ Shea, A. Lawrence, M. Walker, P. (2012). Hygrothermal performance of an experimental hemp–lime building.  
673   *Construction and Building Materials* 36(0), pp.270-275.
- 674   ▪ Shea, A., Wall, K. & Walker, P. (2013). Evaluation of the thermal performance of an innovative pre-fabricated  
675   natural plant fibre building system. *Building Services Engineering Research and Technology*, 34(4), pp. 369-380.
- 676   ▪ Simonson, C.J., Salonvaara, M., Ojanen, T. (2002). The effects of structures on indoor humidity—possibility to  
677   improve comfort and perceived air quality, *Indoor Air* 12, pp.243–251.

- 678     ▪ Simonson, C.J., Salonvaara, M., Ojanen, T. (2004). Heat and Mass Transfer between Indoor Air and a Permeable  
679           and Hygroscopic Building Envelope: Part I – Field Measurements. *Journal of Thermal Envelope and Building*  
680           *Science* 28(1), pp.63-101.
- 681     ▪ Steeman, M., Janssens, A., De Paepe, M. (2009). Performance evaluation of indirect evaporative cooling using  
682           whole-building hygrothermal simulations, *Applied Thermal Engineering* 29, pp.2870–2875.
- 683     ▪ Sutton, A., Black, D., Walker, P. (2011). Natural fibre insulation - An introduction to low-impact building materials,  
684           BRE Information Paper: IP18/11, Building Research Establishment (BRE), UK.
- 685     ▪ Wei, K., Lv, C., Chen, M., Zhou, X., Dai, Z., Shen, D. (2015). Development and performance evaluation of a new  
686           thermal insulation material from rice straw using high frequency hot-pressing, *Energy and Buildings* 87, pp.116–  
687           122.
- 688     ▪ Zach, J., Korjenic, A., Petranek, V., Hroudova, J., Bednar, T. (2012). Performance evaluation and research of  
689           alternative thermal insulations based on sheep wool, *Energy and Buildings* 49, pp.246–253.
- 690     ▪ Zhou, X., Zheng, F., Li, H., Lu, C. (2010). An environment-friendly thermal insulation material from cotton stalk  
691           fibers, *Energy and Buildings* 42, pp.1070–1074.
- 692     ▪ Vololonirina, O., Coutand, M., Perrin, B. (2014), Characterization of hygrothermal properties of wood-based  
693           products – Impact of moisture content and temperature, *Construction and Building Materials* (63), pp.223-233.
- 694     ▪ Woloszyn, M., Kalamees, T., Abadie, M.O., Steeman, M., Kalagasidis, S.A. (2009). The effect of combining a  
695           relative-humidity-sensitive ventilation system with the moisture-buffering capacity of materials on indoor climate  
696           and energy efficiency of buildings, *Building and Environment* 44, pp.515–524.